

GENERALIZATION OF EMBEDDED MULTIPLE DESCRIPTION SCALAR QUANTIZERS YIELDING EMBEDDED UNIFORM CENTRAL QUANTIZERS

**A. I. Gavrilescu, A. Munteanu, J. Cornelis, P. Schelkens*

Vrije Universiteit Brussel

Interdisciplinary Institute for Broadband Technology (IBBT)

Dept. of Electronics and Information Processing (ETRO)

*e-mail: aigavril@etro.vub.ac.be

ABSTRACT

Nowadays Multiple Description Coding (MDC) has become an appropriate approach for efficient transmission over error prone and erasure channels. Additionally, data transmission over variable-bandwidth channels requires the source adaptation to available bit-rate and user's needs; hence a fine grain scalability of each description is a desirable feature. In this context, a new framework enabling the design of generalized Embedded Multiple Description Scalar Quantizers (EMDSQ) yielding embedded uniform central quantizers is proposed in this paper. The design is formulated for an arbitrary number of descriptions. A control mechanism enabling redundancy tuning between the descriptions for each distinct quantization level is also designed. Instantiations of the proposed EMDSQ are employed in a wavelet-based coding system and the redundancy control mechanism is practically demonstrated. Experiments show that multiple description coding systems employing EMDSQ provide state-of-the-art results.

1. INTRODUCTION

Error resilient source coding has become more important as the demand for efficient communication over error-prone and erasure channels - e.g. packet networks, low-power wireless links - has recently increased. In this context, Multiple Description Coding (MDC) is an appropriate approach enabling a good quality data-reproduction from subsets of the transmitted stream.

A desirable feature for image and video transmission over variable-bandwidth channels is the source adaptation to the available bit-rate and user's needs; hence, a fine-grain scalability of each description is essential. Additionally, in contrast to classical non-scalable MDC, the fine-grain scalability of each distinct description features an enhanced error resilience by enabling for the central reconstruction using the available data from partially damaged or partially received descriptions. In this case the decoder can perform the central reconstruction provided that the error or the missing data is localized, within the received data, using techniques such as synchronization markers.

An MDC system allowing for rate control by employing multiple description uniform scalar quantizers (MDUSQ) and bit-plane progressive encoding of each description was proposed in [1]. However, the system is limited to the overall control of redundancy and is conceived only for two descriptions.

In order to provide an arbitrary number of fine-grain refinable (layered) descriptions, we have recently proposed embedded

quantizers for MDC (EMDSQ) in [2], [3], [4]. The major advantage of the EMDSQ is that the central quantizers are uniform at each quantization level, whereas the embedded MDUSQ of [1] are uniform only at the highest rate. This significantly improves the rate-distortion performance [2], [3], [4]. However, the proposed EMDSQ from [2] and [3] are restricted to a fixed high-level overall redundancy.

In this paper, a new framework enabling for the designing of generalized uniform EMDSQ is proposed. All the previously proposed embedded quantization methods for MDC [2], [3], [4] are seen as instantiations of the proposed framework. A control mechanism enabling redundancy tuning between the descriptions for each distinct quantization level is also proposed.

The paper is structured as follows. Section 2 presents a generalized embedded Index Assignment (IA) enabling the design of a wide range of embedded quantizers for MDC. In Section 3, we establish the conditions to be satisfied by the generalized embedded IA to yield uniform embedded central quantizers. The redundancy control mechanism is illustrated in Section 4 and experimental results are given in Section 5. Finally, Section 6 draws the conclusions of this work.

2. GENERALIZED EMBEDDED IA

Let us denote by $Q_m^0, Q_m^1, \dots, Q_m^P$ a set of embedded side quantizers corresponding to an arbitrary number of descriptions M and by Q^0, Q^1, \dots, Q^P the corresponding set of embedded central quantizers, where $Q^{p-1}(\mathbf{q}_1^p, \dots, \mathbf{q}_M^p) = \bigcap_{m=1}^M Q_m^{p-1}(\mathbf{q}_m^p)$ for any quantization level p , $0 \leq p \leq P$ and m , $0 \leq m \leq M$. The embedded side quantizer index $\mathbf{q}_m^p = (q_m^p, q_m^{p-1}, \dots, q_m^0)$ is the output $Q_m^p(x)$ for a source sample $x \in \mathbb{R}$ [5]. For any p , $0 \leq p \leq P$, the partition cells of any quantizer Q_m^p and Q^p are embedded in the partition cells of the quantizers Q_m^p, \dots, Q_m^{p+1} and Q^p, \dots, Q^{p+1} respectively.

Consider an M -dimensional IA matrix \mathbf{M} in which a number N of elements are mapped. We recursively split the IA hypermatrix along each dimension m , $0 \leq m \leq M$ for a number of P levels. According to this recursive splitting \mathbf{M} is a block hypermatrix of the form: $\mathbf{M} = [\mathbf{B}_{j_1 \dots j_m}^p]_{1 \leq j_m \leq J_m^p}$ for any arbitrary level p , $0 \leq p \leq P$, where J_m^p represents the number of block elements at level p for the dimension m . Such an \mathbf{M} hypermatrix can be considered as a generalized embedded IA. Consequently, a set of embedded side quantizers Q_m^p and the corresponding set of central quantizers Q^p are associated with such an embedded IA. It is noticeable that a number of J_m^p cells are contained in Q_m^p ,

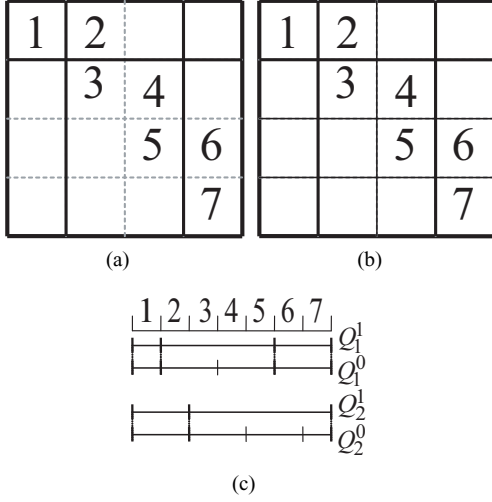


Fig. 1. Index assignment matrix and embedded index allocation corresponding to two-level embedded side quantizers.

additionally, in the most generic case, the number of partitions J_m^p along different dimensions m is not necessarily constant.

Fig. 1 depicts an example of embedded IA matrix ($M = 2$). For the coarsest level ($p = P$), the original IA matrix is a block matrix split into six blocks (two rows and three columns of blocks) as shown in Fig. 1(a). The corresponding side quantizers are depicted in Fig. 1(c) as Q_1^1 and Q_2^1 . For the finer quantization level, each row and column of blocks are either not split or further split into two or three rows or columns of blocks, respectively. The corresponding side quantizers for this level are Q_1^0 and Q_2^0 .

It can be easily verified that the proposed generalized embedded IA includes the particular embedded IAs of multiple description uniform embedded quantization that we proposed in [2], [3], [4] and the embedded MDUSQ proposed by Guionnet et. al. in [1].

3. UNIFORM EMBEDDED CENTRAL QUANTIZERS

As previously indicated in the literature, a uniform entropy coded quantizer with centroid codewords is optimal for high-rates [6] and very nearly optimal for low rates [7]. These conditions were extended for multiple description coding in [8].

The theorem hereunder sets the conditions to be satisfied by the generalized embedded IA to yield Uniform Embedded Central Quantizers. Denote by $[0]$ the zero hypermatrix, and define the operator $nnz(\mathbf{M})$ determining the number of nonzero elements contained in a hypermatrix \mathbf{M} .

Theorem: Let \mathbf{M} be an embedded IA hypermatrix, and the corresponding central quantizer for the highest rate ($p = 0$) be uniform. The central quantizers are uniform at all quantization levels ($p, 0 \leq p \leq P$) if and only if for any p in each hyperblock $\mathbf{B}_{j_1 \dots j_m}^p \neq [0]$ ($1 \leq j_m \leq J_m, 1 \leq m \leq M$) a constant number of consecutive elements are mapped.

Proof: (if) If, for any p , consecutive indices are mapped in any block $\mathbf{B}_{j_1 \dots j_m}^p \neq [0]$, then the corresponding central-quantizer cells are connected cells of size $nnz(\mathbf{B}_{j_1 \dots j_m}^p) \cdot \Delta_C$, where $\Delta_C \in \mathbb{R}_+^*$ is the central-description's constant partition

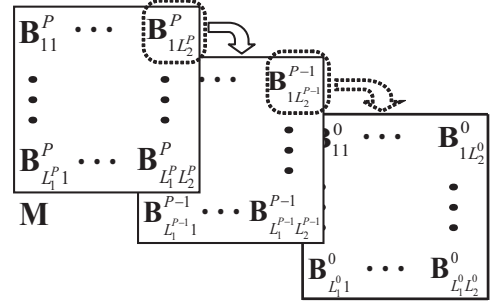


Fig. 2. Recursive block-matrix decomposition.

size for level $p = 0$. By assumption, the number of nonzero elements for all $\mathbf{B}_{j_1 \dots j_m}^p \neq [0]$ at each p is constant, thus: $nnz(\mathbf{B}_{j_1 \dots j_m}^p) = nnz(\mathbf{B}_{i_1 \dots i_m}^p), \forall j_m, i_m, 1 \leq j_m, i_m \leq J_m^p$ for any $\mathbf{B}_{j_1 \dots j_m}^p \neq [0], \mathbf{B}_{i_1 \dots i_m}^p \neq [0]$ and $0 \leq p \leq P$. Hence, the central quantizer at any level p is uniform with the cell size given by $\Delta_C^{(p)} = nnz(\mathbf{B}_{j_1 \dots j_m}^p) \Delta_C$.

(only if) Assume by contradiction that there is $\mathbf{B}_{j_1 \dots j_m}^p \neq [0]$ for which the indices mapped in $\mathbf{B}_{j_1 \dots j_m}^p$ are not consecutive. This implies that the corresponding central-quantizer cell is disconnected, which contradicts the assumption that the central quantizer is uniform at any p . Additionally, for any $\mathbf{B}_{j_1 \dots j_m}^p \neq [0]$, the size of the central-quantizer cell is given by $nnz(\mathbf{B}_{j_1 \dots j_m}^p) \cdot \Delta_C$. The assumption that the central quantizer is uniform at every level implies that $nnz(\mathbf{B}_{j_1 \dots j_m}^p) = const.$, for all $\mathbf{B}_{j_1 \dots j_m}^p \neq [0]$ with $1 \leq j_m \leq J_m^p, 1 \leq m \leq M$.

It can be easily verified that the embedded IAs corresponding to the EMDSQs we proposed in [2], [3], [4] are satisfying the conditions of the theorem above; hence, they represent instantiations of the proposed framework.

Consider, in view of simplification, that any of the hyperblocks $\mathbf{B}_{j_1 \dots j_m}^{p+1}$ are split into the same number L_m^p along the dimension m resulting, at lower level p , in a number $\prod_{m=1}^M L_m^p$ of hyperblocks $\mathbf{B}_{i_1 \dots i_m}^p$. According to the above, each hyperblock $\mathbf{B}_{j_1 \dots j_m}^{p+1}$ within \mathbf{M} is a block hypermatrix defined by its blocks $\mathbf{B}_{i_1 \dots i_m}^p$ as follows: $\mathbf{B}_{j_1 \dots j_m}^{p+1} = [\mathbf{B}_{i_1 \dots i_m}^p]_{1 \leq i_m \leq L_m^p, 1 \leq j_m \leq J_m^{p+1}}$. Therefore, if for the coarser quantization level ($p = P$) $J_m^P = L_m^P$, then the side quantizer Q_m^p will contain $J_m^p = \prod_{i=p}^M L_m^i$ cells. The recursive splitting of a bi-dimensional IA is illustrated in Fig. 2.

Consider a block hypermatrix \mathbf{M} at level p , of the form: $\mathbf{M} = [\mathbf{B}_{j_1 \dots j_m}^p]_{1 \leq j_m \leq J_m^p}$. The number of blocks $\mathbf{B}_{j_1 \dots j_m}^p \neq [0]$ contained in \mathbf{M} is determined via the nonzero-blocks operator $nnb(\mathbf{M}, p)$. It is noticeable that the operator $nnb(\mathbf{M}, 0)$ is identical to the operator $nnz(\mathbf{M})$.

Pursuant to this definition and based on the theorem above, for any of the block hypermatrices $\mathbf{B}_{j_1 \dots j_m}^{p+1} = [\mathbf{B}_{i_1 \dots i_m}^p]_{1 \leq i_m \leq L_m^p, 1 \leq j_m \leq J_m^{p+1}}$, the number of hyperblocks $\mathbf{B}_{i_1 \dots i_m}^p$ different from the zero matrix is constant, and given by $N_p = nnb(\mathbf{B}_{j_1 \dots j_m}^{p+1}, p)$. Additionally, at level $p = P$, $N_P = nnb(\mathbf{M}, P)$ represents the number of hyperblocks $\mathbf{B}_{j_1 \dots j_m}^P \neq [0]$ within \mathbf{M} . The total number of indices mapped in each hyperblock $\mathbf{B}_{j_1 \dots j_m}^p$ is $nnz(\mathbf{B}_{j_1 \dots j_m}^p) = \prod_{i=0}^p N_i$. It can be subsequently shown that the analytical expression of the central EMDSQ for any level

$p, 0 \leq p \leq P$ is:

$$Q^p(x) = \text{sign}(x) \left\lfloor \frac{|x|}{\Delta_C \cdot \prod_{i=0}^p N_i} \right\rfloor \quad (1)$$

The number of partition cells contained in Q^p is $J_p = \prod_{i=1}^P N_i$.

4. REDUNDANCY CONTROL

Denote by R_m the rates and by $D_m(R_m)$ the corresponding side-description distortions. Also, denote by D_0 the central distortion. In single-description coding (SDC) one minimizes D_0 for a given rate R_0 . The redundancy is the bit-rate sacrificed by MDC compared to SDC in order to achieve the same central D_0 distortion:

$$\rho = \frac{\sum_{m=1}^M R_m - R_0}{R_0} \quad (2)$$

From (2) one can deduct the analytical expression of the normalized redundancy:

$$\rho = \frac{\sum_{m=1}^M R_m}{R_0} - 1 \quad (3)$$

In our case, for multiple description embedded quantization, the corresponding side-description rate is of the form $R_m = \log_2(\prod_{i=p}^P L_m^i)$ and $R_0 = \log_2(\prod_{i=p}^P N_i)$. Thus, from (3) we obtain the normalized redundancy:

$$\rho_p = \frac{\sum_{m=1}^M \log_2(\prod_{i=p}^P L_m^i)}{\log_2(\prod_{i=p}^P N_i)} - 1 \quad (4)$$

We can conclude that, for any EMDSQ instantiation, the redundancy is directly dependent on the quantization level p . In addition, the redundancy can be controlled at each distinct quantization level via the N_p and L_p parameters, with $N_p \leq \prod_{m=1}^M L_m^p$.

5. EXPERIMENTS

Performance results for the EMDSQ are presented for a memoryless Gaussian source with zero mean and unit variance (see Figs. 3, 4, 5). The signal-to-noise-ratio (SNR) measure and the normalized redundancy - as expressed by (3) - are used in the above mentioned figures.

In [2] and [3] it was shown that at high redundancies EMDSQ systematically outperformed the state-of-the-art MDUSQ of [1] on a broad set of experiments. Fig. 3 shows comparative EMDSQ and MDUSQ central and side SNR performances for different redundancy levels ($0 \leq \rho \leq 95$). It can be noticed that for $\rho = 0$ both quantizers (i.e. EMDSQ and MDUSQ) show the same performance; meanwhile as the redundancy increases EMDSQ shows ever better central and side SNR results.

In order to demonstrate the redundancy control mechanism, two experiments were performed. In the first experiment - the results of which are given in Fig. 4 - three instantiations of EMDSQ (denoted here as Q_1, Q_2, Q_3) at *different overall redundancy levels* are employed. For the purpose of comparison, for all three EMDSQ instantiations the corresponding central quantizer at $p = 0$ has the same number of cells resulting in an equal overall central distortion. Table 1 indicates the redundancy values at each distinct quantization level (e.g. Q_2 has the overall redundancy $\rho = 0.6$ and five embedded levels ($P = 4$) with maximum

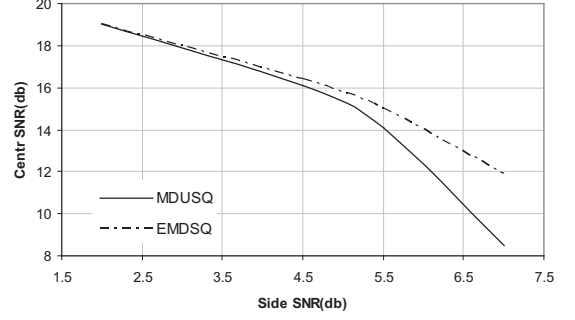


Fig. 3. Comparative side and central SNR performance between EMDSQ and MDUSQ at side $R = 1.2$ at different redundancy levels ($0 \leq \rho \leq 95$) for a memoryless Gaussian source.

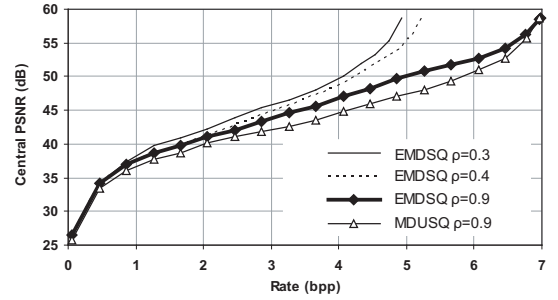


Fig. 6. Comparative central rate-distortion performance obtained on Lena image coded with MD-QT codec employing the EMDSQ and MDUSQ at different overall redundancies.

redundancy for the first four levels ($\rho_p = 1, 1 \leq p \leq 4$) and no redundancy for the last level ($\rho_0 = 0$). For the second experiment - the results of which are given in Fig. 5 - three instantiations of EMDSQ at *the same overall redundancy level* are employed. Table 2 indicates the redundancy values at each distinct quantization level for Q_1, Q_2 , and Q_3 .

Fig. 6 shows the central peak-to-signal-ratio (PSNR) versus the rate obtained with a practical Multiple Description - QuadTree (MD-QT) wavelet based coding system - see [9] - incorporating EMDSQ instantiations operating at different overall redundancies and MDUSQ of [1]. It is important to notice that for EMDSQ it is possible to control the redundancy at each distinct quantization level, while the MDUSQ does not feature this important control mechanism. Also, this example shows that at the same redundancy level, EMDSQ outperforms the state-of-the-art on the whole range of rates.

6. CONCLUSIONS

A new general framework for designing uniform EMDSQ has been proposed in this paper. All the previously proposed embedded quantization methods for MDC [2], [3], [4] are seen as instantiations of the proposed framework. The EMDSQ provides fine-grain refinable descriptions. The conditions to be satisfied by the generalized embedded IA to yield uniform embedded central quantizers are established. In addition, a control mechanism tuning the redundancy between the descriptions for each distinct quantization level is proposed, enabling (1) to control the tradeoff between coding efficiency and resilience to errors, and (2) to improve the resilience

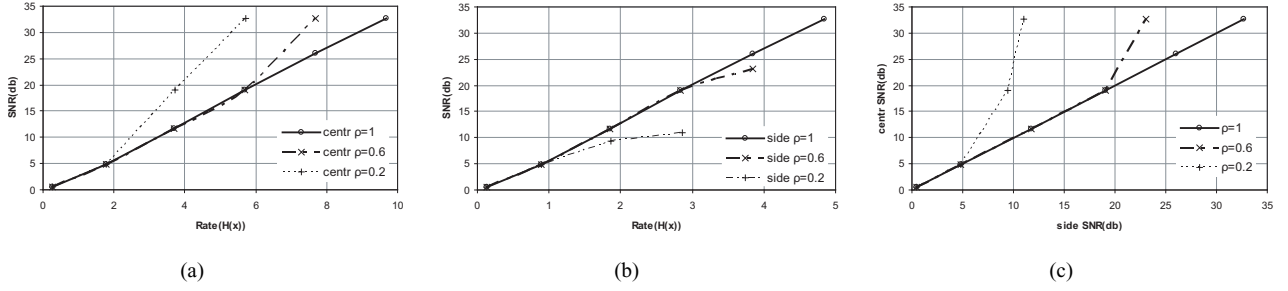


Fig. 4. EMDSQ performance at different overall redundancies for a memoryless Gaussian source (a) Central Rate-distortion (b) Side Rate-distortion (c) Side and Central distortion.

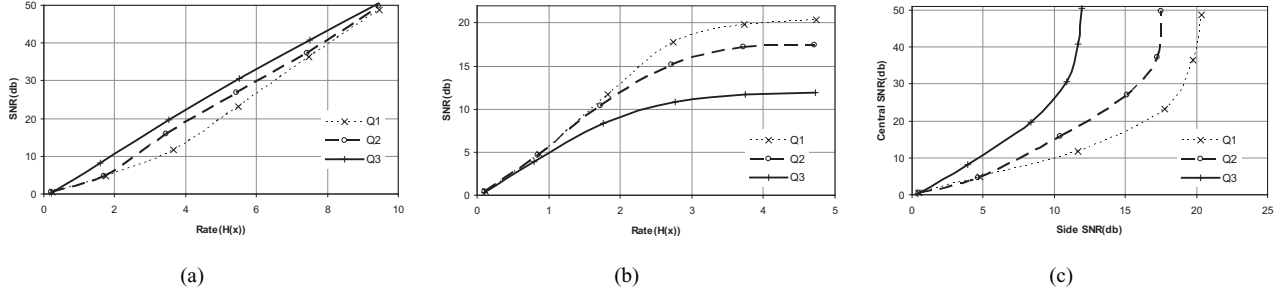


Fig. 5. EMDSQ performances at the same overall redundancy for a memoryless Gaussian source (a) Central Rate-distortion (b) Side Rate-distortion (c) Side and Central distortion.

p	5	4	3	2	1	0
$Q_1(\rho = 1.0)$	1.0	1.0	1.0	1.0	1.0	1.0
$Q_2(\rho = 0.6)$	-	1.0	1.0	1.0	1.0	0.0
$Q_3(\rho = 0.2)$	-	-	1.0	1.0	0.0	0.0

Table 1. The redundancy value at each level p for the EMDSQ instantiations from Fig.4.

p	5	4	3	2	1	0
$Q_1(\rho = 0.25)$	1.0	1.0	1.0	0.6	0.4	0.3
$Q_2(\rho = 0.25)$	1.0	1.0	0.4	0.4	0.3	0.3
$Q_3(\rho = 0.25)$	1.0	0.2	0.2	0.2	0.2	0.2

Table 2. The redundancy value at each level p for the EMDSQ instantiations from Fig.5.

by increasing the redundancy in the important layers of the bit-stream. Finally, experimental results demonstrate the redundancy control mechanism and show that EMDSQ instantiations outperform the state-of-the-art.

7. ACKNOWLEDGEMENTS

This work was supported by the Federal Office for Scientific, Technical and Cultural Affairs (IAP-V, Mobile Multimedia). P. Schelkens and A. Munteanu have post-doctoral fellowships with the Fund for Scientific Research, Flanders (FWO).

8. REFERENCES

[1] T. Guionnet, C. Guillemot, and S. Pateux, "Embedded multiple description coding for progressive image transmission over unreliable channels," in *IEEE Int. Conf. Image Proc., ICIP'01*, 2001, pp. 94 – 97.

[2] A. I. Gavrilescu, A. Munteanu, P. Schelkens, and J. Cornelis, "Embedded multiple description scalar quantizers," *IEE Electronics Letters*, vol. 39, no. 13, pp. 979–980, 2003.

[3] A. I. Gavrilescu, A. Munteanu, J. Cornelis, and P. Schelkens, "High-redundancy embedded multiple-description scalar quantizers for robust communication over unreliable channels," in *5th International Workshop on Image Analysis for Multimedia Interactive Services, WIAMIS'04*, Lisboa.

[4] A. I. Gavrilescu, A. Munteanu, J. Cornelis, and P. Schelkens, "A new family of embedded multiple description scalar quantizers," in *IEEE International Conference on Image Processing, ICIP'04*, Singapore, 2004, pp. 159 – 162.

[5] D. Taubman and M.W. Marcelin, *JPEG2000: Image Compression Fundamentals, Standards, and Practice*, Kluwer Academic Publishers, Norwell, Massachusetts, 2002.

[6] H. Gish and J. N. Pierce, "Asymptotically efficient quantizing," *IEEE Trans. Inform. Theory*, vol. 14, pp. 676–683, 1968.

[7] N. Farvardin and J.W. Modestino, "Optimum quantizer performance for a class of non-gaussian memoryless sources," *IEEE Trans. Inf. Theory*, vol. 30, no. 3, pp. 485–497, 1984.

[8] V. A. Vaishampayan and J. Domaszewicz, "Design of entropy-constrained multiple description scalar quantizers," *IEEE Trans. Inform. Theory*, vol. 40, no. 1, pp. 245–250, 1994.

[9] A. I. Gavrilescu, A. Munteanu, J. Cornelis, and P. Schelkens, "Embedded multiple description scalar quantizers and wavelet-based quadtree coding for progressive image transmission over unreliable channels," in *12th European Signal Processing Conference, EUSIPCO'04*, Vienna, 2004, vol. 1, pp. 645 – 648.